CORA Cork Open Research Archive
Cartlann Taighde Oscailte Chorcaí

UCC Library and UCC researchers have made this item openly available. Please let us know how this has helped you. Thanks!

Title	Copper/molybdenum nanocomposite particles as catalysts for the growth of bamboo-structured carbon nanotubes
Author(s)	Li, Zhonglai; Larsson, J. Andreas; Larsson, Peter; Ahuja, Rajeev; Tobin, Joseph M.; O'Byrne, Justin; Morris, Michael A.; Attard, Gary; Holmes, Justin D.
Publication date	2008-07-23
Original citation	Li, Z., Larsson, J. A., Larsson, P., Ahuja, R., Tobin, J. M., O'Byrne, J., Morris, M. A., Attard, G. and Holmes, J. D. (2008) 'Copper/Molybdenum Nanocomposite Particles as Catalysts for the Growth of Bamboo-Structured Carbon Nanotubes', The Journal of Physical Chemistry C, 112(32), pp. 12201-12206. doi: 10.1021/jp8023556
Type of publication	Article (peer-reviewed)
Link to publisher's version	https://pubs.acs.org/doi/10.1021/jp8023556 http://dx.doi.org/10.1021/jp8023556 Access to the full text of the published version may require a subscription.
Rights	**© 2008 American Chemical Society. This document is the Accepted Manuscript version of a Published Work that appeared in final form in The Journal of Physical Chemistry C, copyright © American Chemical Society after peer review and technical editing by the publisher. To access the final edited and published work see https://pubs.acs.org/doi/10.1021/jp8023556**
Item downloaded from	http://hdl.handle.net/10468/8149

Downloaded on 2021-05-08T14:13:48Z

UCC University College Cork, Ireland
Coláiste na hOllscoile Corcaigh

Copper/Molybdenum Nanocomposite Particles as Catalysts for the Growth of Bamboo-Structured Carbon Nanotubes

Zhonglai Li [1], J. Andreas Larsson [2], Peter Larsson [3], Rajeev Ahuja [3], Joseph M. Tobin [1], Justin O'Byrne [1], Michael A. Morris [1,2], Gary Attard [4] and Justin D. Holmes [1,2*]

[1] Department of Chemistry, Materials Section and Supercritical Fluid Centre, University College Cork, Cork, Ireland and Centre for Research on Adaptive Nanostructures and nanodevices (CRANN), Trinity College Dublin, Dublin 2, Ireland.

[2] Tyndall National Institute, University College Cork, Lee Maltings, Prospect Row, Cork, Ireland.

[3] Condensed Matter Theory Group, Department of Physics & Materials Science, Uppsala University, P.O. Box 530, SE-751 21 Uppsala, Sweden.

[4] School of Chemistry, Cardiff University, Main Building, Park Place, Cardiff, CF10 3AT, UK

**To whom correspondence should be addressed Tel: +353 (0)21 4903608; Fax, +353 (0)21 4274097; Email: j.holmes@ucc.ie*

Abstract

Bamboo-structured carbon nanotubes (BCNTs), with mean diameters of 20 nm, have been synthesized on MgO-supported Cu and Mo catalysts by the catalytic chemical vapour deposition of methane. BCNTs could only be generated using a combination of Cu and Mo catalysts. No BCNTs were produced from either individual Cu or Mo catalysts. In combination, Mo was found to be essential for cracking the methane precursor, whilst Cu was required for BCNT formation. Energy dispersive x-ray analysis of the individual particles at the tips of the nanotubes suggest that Cu and Mo are present as a 'composite' nanoparticle catalyst after growth. First-principles modeling has been used to describe the interaction of the Cu/Mo catalyst with the nanotubes suggesting that the catalyst binds with the same energy as traditional catalysts such as Fe, Ni and Co.

Introduction

Carbon nanotubes (CNTs) have attracted considerable interest in recent years due to their remarkable electrical, mechanical, and thermal properties and their potential applications in nanoelectronics, sensors and as catalyst supports. [1-9] There have been a significant number of reports on the synthesis of CNTs, including single-walled and multi-walled CNTs, using Fe, Co and Ni-containing catalysts. [10-14]

Cu is believed to be inactive for the decomposition of methane in the traditional catalytic system. However, it is incorrect to think that copper has no hydrocarbon reforming capability because its role as an active catalyst in hydrocarbon fuel cells is well known. [15,

[16] Carbon fibres, with diameters as large as 200 nm, have been prepared by methane pyrolysis over Cu particles supported on an alumina substrate. In another study, bamboo-structured carbon fibres were grown on Cu particles, with a mean diameter of 200 nm, at temperatures between 960 and 1018 °C.[17] Carbon fibers have also been prepared on K-promoted Cu catalysts, where it was suggested that the K acts as an electron dopant to Cu in the pyrolysis of acetylene.[18] Mo is often studied as a promoter for Fe, Co and Ni catalysts for the generation of CNTs, leading to improved yields. [19-25] For example, Liu *et al.* [26] showed that the yield of single-walled carbon nanotubes (SWNTs) from an Fe/MgO catalyst was less than 25 wt% relative to the weight of the catalyst, even when the loading of Fe salts was as high as 40 wt% with regard to the weight of MgO. In contrast, the yield of CNTs was increased up to 120 wt%, relative to the weight of catalyst, when a small amount of Mo salt was added to the Fe catalyst as a promoter. However, supported Mo catalysts have been shown to form molybdenum carbide, not CNTs, when using hydrocarbons such as methane and butane as a carbon feedstock at temperatures greater than 700 °C. [27-30]

Recently, Cu, Ag and Au nanoparticles, supported on Si wafers, were used as catalysts for the production of SWNTs, [31,32] These results contradict the accepted mechanisms of CNT growth, where only significant yields of CNTs are produced from transition element catalysts such as Fe, Co and Ni. In this paper we show that MgO-supported Cu/Mo catalysts can generate bamboo-structured carbon nanotubes (BCNTs) by the direct catalytic chemical vapor deposition (CCVD) of methane. Density functional theory (DFT) calculations have been performed for Cu, Mo and Cu/Mo particles bonded to a

CNT to determine how Cu and Mo interact with the nanotubes. We show that the catalytic metal particles must, in addition to decomposing the carbon feed-stock gas and seeding the formation of graphitic caps on the surface, be able to stabilize the growing end of the CNTs.[33] This growth requisite requires that the CNT – metal particle binding energies are large enough to maintain the hollow tube structure, and is thus relevant for the growth of both single-walled and multi-walled CNTs.

Experimental

Synthesis of Bamboo-Structured Carbon Nanotubes

BCNTs were synthesized by CCVD of methane over Cu/Mo catalysts supported on MgO. The catalysts were formed by impregnating the MgO support with aqueous solutions of $Cu(NO_3)_2.6H_2O$ and $(NH_4)Mo_6O_{24}.H_2O$. The mixture was sonicated for 30 min and dried at 100 ºC overnight. The dried powder was sintered at 500 ºC for 6 h to produce the catalyst. The metal content of the catalyst was recorded as a weight percent with regard to the MgO support. 0.3 g of the catalyst was placed in a quartz tube in a tube furnace (20 mm ID). The catalyst was reduced by heating to 850 ºC in a H_2/Ar flow (20/180 ml min^{-1}) for 30 min. Methane was then fed into the quartz tube at a flow rate of 100 ml min^{-1} for 60 min after which time the furnace was cooled to room temperature. To isolate BCNTs from the carbon material generated during the reaction, and remove the metal catalyst particles, the carbon/catalyst powder was treated with 3 M HNO_3 and washed with water.

Characterization of Carbon Nanotubes

Scanning electron microscopy (SEM) was performed on a LEO 1530EP scanning microscope. Transmission electron microscopy (TEM) was conducted on a FEI Tecnai F20 (super TWIN lens) operating at 200 kV with an EDAX RTEM detector. Samples for TEM analysis were dispersed in ethanol and deposited onto Ni grids. Raman spectra were recorded on a Renishaw 1000 Raman system in an ambient atmosphere using a 5 mW He-Ne laser (λ = 514.5 nm) and a CCD detector.

Theoretical Details

Calculation of Metal – CNT Binding Strengths for Cu, Mo and Cu/Mo Particles

To investigate the ability of Cu/Mo nanoparticles to stabilize and support the growing end of a CNT we have calculated binding energies of a (5,0) SWNT to a M_{13} metal cluster (M = Cu, Mo) with different compositions of Cu and Mo atoms, and compared them to the binding energies of Fe, Co and Ni clusters previously reported. [33] It has been shown that trends in binding energy can be correctly described with a (5,0) SWNT bonded to a thirteen atom metal cluster (M_{13}) [33] that we have used in this study. The binding energies have been calculated with density functional theory (DFT) using the Perdew-Burke-Ernzenhof (PBE) formulation of the generalized gradient approximation (GGA) exchange and correlation functional,[34] in conjunction with a polarized valence triple-zeta (TZVP) basis set [35] and relativistic effective core potentials (ECPs) for Cu and Mo, [36,37] as implemented in the Turbomole program.[38-41] All clusters were fully geometry optimized in the gas phase at 0 K

Results and Discussion

Neither CNTs nor any other forms of solid carbon nanostructures formed when methane was flowed over Cu/MgO catalysts (5 and 10 wt% with respect to MgO) for reaction times of more than 1 h at a temperature of 850 °C (Figure 1a and 1b). The Cu/MgO catalysts had a red appearance upon removal from the furnace due to the formation of metallic Cu nanoparticles on the surface of the MgO. This lack of CNT formation is related to the low activity of Cu for decomposing methane. Similarly, no CNTs were formed from supported Mo catalysts, containing 5 wt% and 10 wt% Mo, with respect to the MgO support. Although Mo is assumed to form small-sized particles on a 5 wt% Mo catalyst, only black particles on the catalyst after CCVD of methane at 850 ºC for 1 h were observed in the TEM images (Figure 1c and 1d). Molybdenum carbide may be formed upon heating the Mo catalyst with a carbon feed-stock gas at high temperatures.[30] However, x-ray diffraction (XRD) analysis of the Mo/MgO catalysts after attempted methane decomposition showed no evidence for the formation of molybdenum carbide, only patterns of MgO were observed in the XRD pattern, possibly due to oxidation of the unstable molybdenum carbide phase when the sample was exposed to air and the high dispersion of molybdenum species on MgO.

The effect of combining Cu and Mo to enhance the formation of CNTs was investigated in detail. When methane was passed over MgO-supported Cu/Mo catalysts at 850 °C for 1 h, no CNTs were observed by TEM when using a 10 wt% Cu - 1wt% Mo catalyst. A low yield of carbon product, approximately 3 wt% relative to the weight of the catalyst was formed at a Mo loading of 3 wt% (Figure 2a and 2b). In contrast, a significant yield

of carbon, 17 wt% with respect to the weight of catalyst, was obtained when the loading of Mo was increased to 5 wt%, at a Cu loading of 10 wt% (Figure 2c). The formation of carbon on the Cu/Mo catalysts was also investigated at a Cu loading of 2 wt% and a Mo loading of 5 wt%, with respect to the MgO support. Only a few CNTs were observed by TEM from the 2 wt% Cu loading. These data clearly show that obtaining the right balance of Cu and Mo in the catalyst is essential for the generation of BCNTs.

SEM data provides further evidence that high yields of BCNTs were obtained at Cu loadings of 5 and 10 wt%, in conjunction with 5 wt% Mo, as shown in Figure 3. The SEM images not only show significant amounts of CNTs protruding from the surface of the catalyst, but metal particles can be clearly observed at the tips of the CNTs. This observation suggests that the CNTs grow through 'root-growth' and/or 'tip-growth'.[13] Much confusion is present in the literature concerning the definition of these terms, but we note that tip-growth and root-growth are essentially the same mechanism, in that growth occurs at the CNT – metal particle interface, with the difference that in the latter case the catalytic metal particles are bound to a substrate surface. This growth mechanism is sometimes referred to as substrate-grown CNTs as opposed to 'floating' catalyst growth, where the catalyst particle is not attached to the substrate surface.

The TEM images shown in Figure 4 were taken of purified CNTs, prepared on a MgO-supported Cu/Mo catalyst (10 wt.% Cu and 5 wt% Mo). 3 M HNO_3 was used to remove both the MgO support and external catalyst particles. The images clearly show CNTs with a uniform outer diameter of 20 nm, having bamboo structures. The walls of the

CNTs were constructed from 10-20 graphitic layers and the inner diameters ranged from 5 to 10 nm.

Catalyst particles were observed at the tips of the CNTs and in some cases small metal particles were seen inside the CNTs, after removal of excess catalyst material, which means that the ends of the BCNTs are closed. Furthermore, TEM analysis showed that some spherical Cu/Mo particles that exist prior to CNT growth become elongated after the formation of BCNTs. This elongation of the nanoparticles must be due to the interaction of the growing BCNT with the catalyst. The change in particle shape from spherical to elliptical leads us to believe that a "plastic" phase of the catalyst particles is reached during BCNT growth, in which the particle shape is changing in a similar manner as was found by Hofmann *et al.* [42] and Lin *et al.* [43] in their *in-situ* observation of catalyst particles during the early stage growth of CNTs. TEM and EDAX analysis of a catalytic nanoparticle at the tip of BCNT are shown in Figure 5. EDAX data suggests that the nanoparticles used to grow the BCNTs are bimetallic in nature, consisting of both Cu and Mo. In the EDAX spectrum shown in Figure 5, the peak at 17.4 keV can be attributed to Mo and the signal at 8.0 keV to the K_α transition for Cu. The peak at 7.4 keV is attributed to the Ni K_α transition from the TEM grid.

A high-resolution TEM image of a catalyst particle after the reaction is shown in Figure 5. The lattice spacing observed in the particle, of *ca.* 0.21 nm, may be attributed to either the Cu (111) or Mo (111) planes, as Cu and Mo have very similar lattice spacings. The lattice distance of *ca.* 0.37 nm between the parallel fringes (layers) is assigned to graphite

carbon sheets indexed as the diffraction plane (002) in Figure 4d. [19] However, the lattice spacing is slightly higher than that of graphite, *i.e.* 0.34 nm, possibly due to the formation of defective carbon nanostructures.

The structure of the BCNTs is indicated by the Raman spectra shown in Figure 5. Two characteristic peaks were observed from the BCNTs. The D-band located at approximately 1326 cm^{-1} is attributed to defects, curved graphite sheets and lattice distortions in the carbon structures. The G-band, at about 1588 cm^{-1}, is characteristic of graphite. The intensity of the D-band is stronger than that of the G-band for all three carbon samples, but the intensity of the 1326 cm^{-1} peak decreases with an increase in the amount of Cu in the catalyst. The intensity ratios between the D-band and G-band (I_D/I_G ratio) were found to be 1.20 for Cu loadings of 10 wt.%, indicating that some defects exist in the structure of the BCNTs.

The mechanism by which CNTs grow from transition elements such as Fe, Co and Ni is well studied, but the growth mechanism associated with the growth of CNTs from a composite catalyst of two metals is still unclear, especially when in our process Cu and Mo alone do not result in the formation of CNTs. Using DFT we have modeled the interaction between Cu/Mo composite nanoparticles and the (5,0) SWNT to develop an understanding of how, when combined, Cu and Mo actively generate BCNTs. Fe, Ni and Co are known to have larger binding energies to CNTs compared with Cu, Pd and Au, with the former binding energies being close in energy to the carbon dangling bond energy of the corresponding SWNT open end.[33] Since a CNT open end is unstable it

needs to be stabilized during growth by the catalytic metal particle, which is one of the fundamental tasks of the catalyst, in addition to decomposing the carbon feed-stock gas and seeding the formation of the graphitic caps on the surface. The metal – CNT binding strength needs to be balanced to match the CNT open end carbon dangling bond energy. [33, 44] For the M_{13} cluster – (5,0) SWNT complex, the binding energies for M = Fe, Ni and Co are slightly larger than the (5,0) SWNT open end dangling bond energy. The open end carbon dangling bond energy is 2.76 eV with PBE/TZVP. For the Cu_{13} cluster – (5,0) SWNT complex **I** (see Figure 7a) we get a binding energy (per carbon atom at the open end) of 2.29 eV, which is close to the value reported by Ding *et al.* [33] (2.46 eV) using a planewave basis. The binding energy for the Mo_{13}-(5,0) complex **II** is 3.63 eV. When all of the Cu atoms of the Cu_{13} particle that are not bonded to the nanotube are replaced by Mo **III** (Mo_7Cu_6, see Figure 7b), the binding energy is only slightly lowered to 2.05 eV. Also replacing the central Cu of complex **I** by Mo **IV** ($MoCu_{12}$) leads to a lowering of the binding energy to 1.73 eV. The lowering is, however, partly artificial, since $MoCu_{12}$ is greatly stabilized by forming a closed-shell electronic state, which decreases the calculated binding energy. This effect would be less pronounced at high temperatures (DFT calculations are done at 0 K), and also for larger clusters. The results for **III** and **IV** show that Cu coating of Mo gives particles that, compared to Cu particles, have the same, or slightly decreased, ability to stabilize the growing end of a CNT (i.e. too low a binding energy). If on the other hand, there is Mo dopants in the surface layer of Cu particles, modelled by replacing the *side* **V**, or *top* **VI** (both with stoichiometry $MoCu_{12}$) Cu atom of complex **I** by Mo, then the binding energy increases, compared to **I**, to 2.35 eV for the **V** and 2.90 eV for the **VI** complex. The increase in binding energy is

quite large for the 'top' position, and a similar increase (2.76 eV) was computed when the *top* Cu atom of **III** was replaced by Mo **VII** (Mo_8Cu_5). These latter binding energies are at a par with the open end dangling bond energy, as was also found for Fe, Ni and Co [33]. This means that a composite nanoparticle containing both Cu and Mo would be able to stabilize a CNT growing end. It would, however, not be favourable to have too much Mo, since Mo binds carbon too strongly, thus making Mo-C bonds more favourable than C-C bonds.

Our analysis has shown that BCNTs are produced on Cu/Mo catalyst particles, which our theoretical calculations show have metal – CNT binding energies that are in the correct range to support the growth of CNTs. We show from the absence of BCNT growth from pure Mo particles, and also from particles with small Cu/Mo ratios, that Mo alone does not catalyze CNT growth. When the Cu/Mo ratio is increased to 1 – 2 a high yield of CNT product is produced, thus a significant amount of Cu is essential for the formation of CNTs. It is also clear from the inactivity of pure Cu particles that Mo is needed for the decomposition of the carbon feed-stock gas. Thus, we have shown that both pure Mo and pure Cu particles are inactive at catalyzing CNT growth. It is only when Cu and Mo are combined into composite nanoparticles that BCNTs are produced. Our theoretical calculations using DFT explain these observations, in that Cu particles have too weak binding strengths to stabilize the CNT hollow open-end, and that Mo particles have too strong binding strengths to favor the formation of C-C bonds over C-Mo bonds, *i.e.* no carbon nanostructures are formed from pure Mo. Contrary to pure particles, our calculations show that Cu/Mo composite particles have binding strengths that would

support CNT growth. Considering the ratios between Cu and Mo in the preparation of successful catalyst particles, it is reasonable to assume that these particles have near equal amounts of the two metals. Another possible scenario is that the particles that produce CNTs are Cu particles with a small percentage of Mo, but that the formation of such particles are only produced in big enough quantities at much higher ratios of Mo due to the difficulty of alloying Cu and Mo, *i.e.* Mo doped Cu particles could be the active catalyst. There is no evidence of domains in the active catalyst particles, as we have found no grain boundaries in the TEM images, but since Mo and Cu are so close in lattice spacing we are not ruling out that they contain Cu and Mo domains that are not in the form of grains.

The Cu/Mo catalyst particles grow BCNTs in which the particles adjust their shape to the graphitic structure that is grown with elongation and contraction at periodic intervals. In the growth of SWNTs and MWNTs it has been shown that such an elongation followed by a contraction of the catalytic particles happens at the very start of the tube growth.[42-43] We suggest that the repetition of this behavior in our case is connected to the presence of Mo and its high affinity to carbon. It is probable that Mo atoms/clusters at the surface of the particles create adhesion points for the particles to the inside of the bamboo compartments, which are only broken at maximum particle elongation and stress.

Conclusions

BCNTs have been synthesized from a composite Cu/Mo catalyst supported on MgO. EDAX analysis of the individual catalyst nanoparticle of 20 nm in diameter at the tip of

CNTs indicates that both Cu and Mo elements co-exist as a composite nanoparticle catalyst for the growth of CNTs. The modeling of CNT growth on a composite catalyst nanoparticle including Cu and Mo suggests that Mo binds to the surface of the Cu, forming Mo carbide by the reaction of Mo and CH_4, supplying the needed carbon species to the Cu particle for growth.

Acknowledgements

The authors acknowledge the European Union under the DESYGN-IT project (STREP Project 505626-1), Nanocage (Marie Curie Early Stage Training Network MEST-CT-2004-506854), the Tyndall National Access Programme (NAP Project 108), and the Swedish Research Council. Z.L. thanks Dr Uwe for SEM measurements. The authors would like to thank Gregory Goodlett and Johnson Matthey for supplying the EDX data.

References

1. Iijima, S. *Nature* **1991**, *354*, 56.
2. Ebbensen, T. W. *Phys. Today* **1996**, *49*, 26.
3. Wong, S. S.; Harper, J. D.; Lansbury, P. T., Jr.; Lieber, C. M. *J. Am. Chem. Soc.* **1998**, *120*, 603.
4. Wang, M. S.; Peng, L.-M.; Wang, J. Y.; Chen, Q. *J. Phys. Chem. B.* **2005**, *109*, 110.
5. Heller, I.; Kong, J.; Heering, H. A.; Williams, K. A.; Lemay, S. G.; Dekker, C. *Nano Lett.* **2005**, *5*, 137.
6. Ito, T.; Sun, L.; Henriquez, R. R.; Crooks, R. M. *Acc. Chem. Res.* **2004**, *37*, 937.
7. Yoo, E.; Gao, L.; Komatsu, T.; Yagai, N.; Arai, K.; Yamazaki, T.; Matsuishi, K.; Matsumoto, T.; Nakamura, J. *J. Phys. Chem. B.* **2004**, *108*, 18903,
8. Bekyarova, E.; Davis, M.; Burch, T.; Itkis, M. E.; Zhao, B.; Sunshine, S.; Haddon, R. C. *J. Phys. Chem. B.* **2004**, *108*, 19717,.
9. Xing, Y. *J. Phys. Chem. B.* **2004**, *108*, 19255,
10. Jung, Y. J.; Wei, B. Q.; Vajtai, R.; Ajayan, P. M.; Homma, Y.; Prabhakaran, K.; Ogino, T. *Nano Lett.* **2003**, *3*, 561.
11. Huang, S.; Cai, X.; Du, C.; Liu, J. *J. Phys. Chem. B.* **2003**, *107*,13251.
12. Ciuparu, D.; Chen, Y.; Lim, S.; Haller, G. L.; Pfefferle, L. *J. Phys. Chem. B.* **2004**, *108*, 503.
13. Kim, N. S.; Lee, Y. T.; Park, J.; Han, J. B.; Choi, Y. S.; Choi, S. Y.; Choo, J.; Lee, G. H. *J. Phys. Chem. B.* **2003**, *107*, 9249.

14. Li, Y.; Kinloch, I. A.; Shaffer, M. S. P.; Singh, C.; Geng, J.; Johnson, B. F. G.; Windle, A. H. *Chem. Mater.* **2004**, *16*, 5637.

15. Horita, T., Yamaji, K., Kato, T., Sakai, N., Yokokawa H., *Solid State Ionics*, **2004**, *169*, 105.

16. Liao, M., Au, C., Ng, C. *Chem. Phys. Lett.* **1997**, *272*, 445.

17. Farmer, B., Holmes, D., Vandeperre, L., Stearn, R., Clegg, W., MRS fall meeting on nanomaterials for structural applications, Warrendale, PA, Boston, **2002**, p 81

18. Tao, X.; Zhang, X.; Cheng, J.; Wang, Y.; Liu, F.; Luo, Z. *Chem. Phys Lett*, **2005**, *409*, 89.

19. Li, Y.; Liu, J.; Wang, Y.; Wang, Z. L. *Chem. Mater*. **2001**, *13*, 1008.

20. Jodin, L.; Dupuis, A. C.; Rouviere, E.; Reiss, P. *J. Phys. Chem. B.* **2006**, *110*, 7328.

21. Alvarez, W. E.; Pompeo, F.; Herrera, J. E.; Balzano, L.; Resasco, D. E. *Chem. Mater.* **2002**, *14*, 1853.

22. Wang, B.; Wei, L.; Yao, L.; Li, L. J.; Yang, Y.; Chen, Y. *J. Phys. Chem. C.* **2007**, *111*, 14612.

23. Saito, T.; Ohshima, S.; Xu, W. C.; Ago, H.; Yumura, M.; Iijima, S. *J. Phys. Chem. B.* **2005**, *109*, 10647.

24. Zhou, L.; Ohta, K.; Kuroda, K.; Lei, N.; Matsuishi, K.; Gao, L.; Matsumoto, T.; Nakamura, J. *J. Phys. Chem. B.* **2005**, *109*, 4439.

25. Deng, W.; Xu, X.; Goddard, W. A., III . *Nano Lett.* **2004**, *4*, 2331.

26. Li, Q.; Yan, H.; Cheng, Y.; Zhang, J.; Liu, Z. *J. Mater. Chem.* **2002**, *12*, 1179.

27. Wu, W., Wu, Z., Liang, C., Ying, P., Feng, Z., Li, C. *Phys. Chem. Chem. Phys*. **2004**, *6*, 5603.

28. Ding, W.; Li, S.; D Meitzner, G.; Iglesia, E. *J. Phys. Chem. B.* **2001**, *105;* 506.

29. Oshikawa, K.; Nagai, M.; Omi, S. *J. Phys. Chem. B.* **2001**, *105*, 9124.

30. Xiao, T.; York, A. P. E.; Williams, V. C.; Al-Megren, H.; Hanif, A.; Zhou, X.; Green, M. L. H. *Chem. Mater*. **2000**, *12*, 3896.

31. Takagi, D.; Homma, Y.; Hibino, H.; Suzuki, S.; Kobayashi, Y. *Nano Lett.* **2006**, *6*, 2642.

32. Bhaviripudi, S.; Mile, E.; Steiner, S. A., III; Zare, A. T.; Dresselhaus, M. S.; Belcher, A. M.; Kong, J. *J. Am. Chem. Soc*. **2007**, *129*, 1516.

33. Ding, F.; Larsson, P.; Larsson, J. A.; Ahuja, R.; Duan, H.; Rosén, A.; Bolton, K. *Nano Lett*, **2008**, *8*, 463.

34. Perdew, J. P.; Burke, K.; Ernzerhof, M. *Phys. Rev. Lett*. **1996**, *77*, 3865.

35. Schäfer, A.; Huber, C.; Ahlrichs, R. *J. Chem. Phys*. **1994**, *100*, 5829.

36. Andrae, D.; Haeussermann U.; Dolg, M.; Stoll H.; Preuss, H. *Theor. Chim. Acta* **1990**, *77*. 123.

37. Dolg, M.; Wedig, U.; Stoll, H.; Preuss, H. *J. Chem. Phys*. **1987**, *86*, 866.

38. Treutler, O.; Ahlrichs, R. *J. Chem*. *Phys*. **1995**, *102*, 346.

39. Arnim, M. v.; Ahlrichs, R. *J. Comp. Chem*. **1998**, *19*, 1746.

40. Eichkorn, K.; Treutler, O.; Öhm, H.; Häser, M.; Ahlrichs, R.; *Chem. Phys. Lett*. **1995**, *240*, 283.

41. Ahlrichs, R.; Bär, M.; Häser, M.; Horn, H.; Kölmel, C. *Chem, Phys. Lett*. **1989**, *162*, 165.

42. Hofmann, S.; Sharma, R.; Ducati, C.; Du, G.; Mattevi, C.; Cepek, C.; Cantoro, M.; Pisana, S.; Parvez, A.; Cervantes-Sodi, F.; Ferrari, A. C.; Dunin-Borkowski, R.; Lizzit, S.; Petaccia, L.; Goldoni, A.; Robertson, J. *Nano Lett.* **2007**, *7*, 602.

43. Lin, M.; Tan, J. P. Y.; Boothroyd, C.; Loh, K. P.; Tok, E. S.; Foo, Y. L. *Nano Lett*. **2007**, *7*, 2234.

44. Larsson, P.; Larsson, J. A.; Ahuja, R.; Ding, F.; Yakobson, B. I.; Duan, H.; Rosén, A.; Bolton, K. *Phys. Rev. B*, **2007**, *75*,115419.

Figures

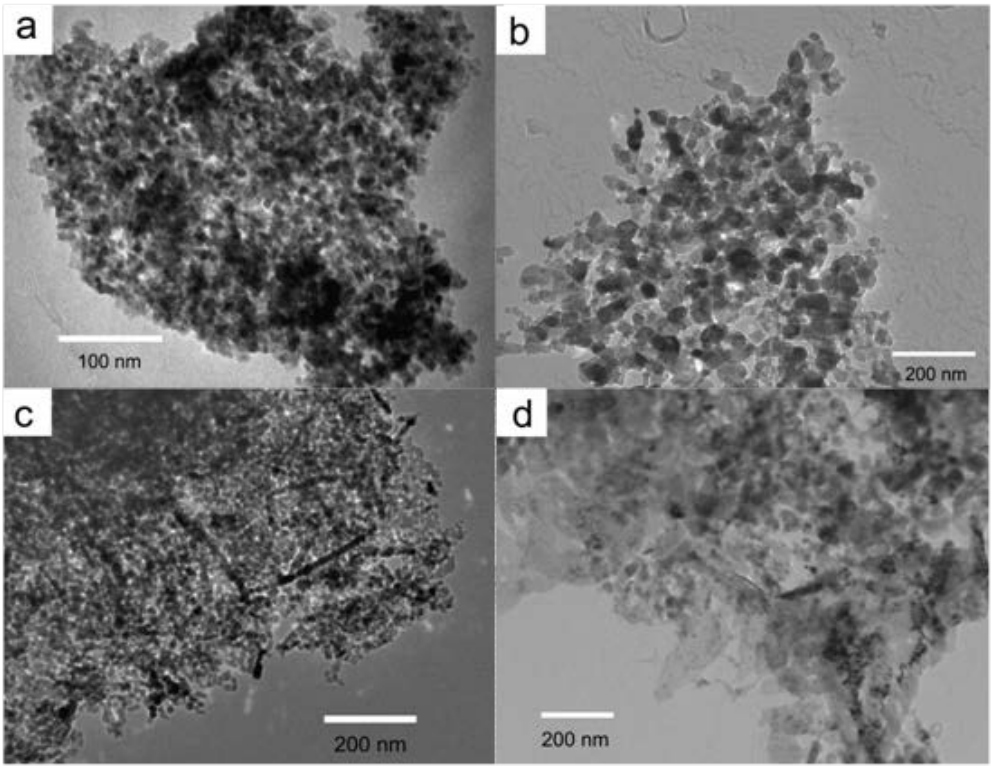

Figure 1. TEM images of catalysts after reaction with methane at 850 ºC for 1 h: (a) 5 wt% Cu/MgO, (b) 10wt% Cu/MgO, (c) 5wt% Mo/MgO and (d) 10 wt% Mo/MgO.

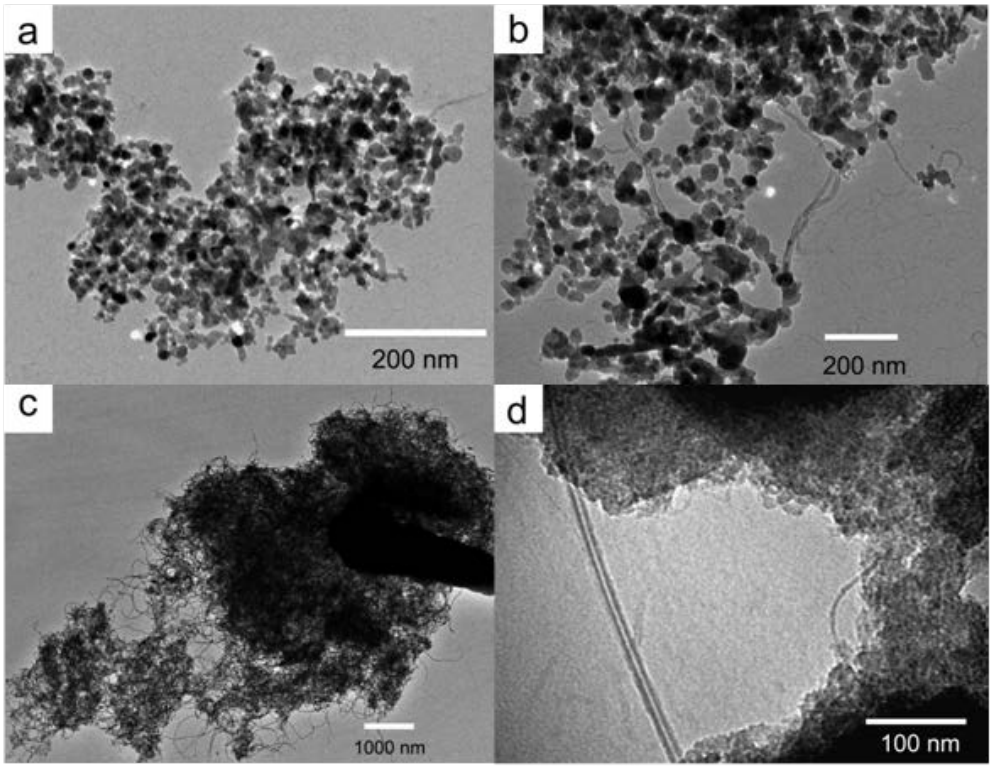

Figure 2. TEM images of carbon nanotubes prepared on: (a) 1 wt% Mo -10 wt% Cu/MgO, (b) 3 wt% Mo -10 wt% Cu/MgO, (c) 5 wt% Mo – 10 wt% Cu/MgO (d) 2wt% Cu - 5wt% Mo/MgO, at 850 ^{o}C for 1h.

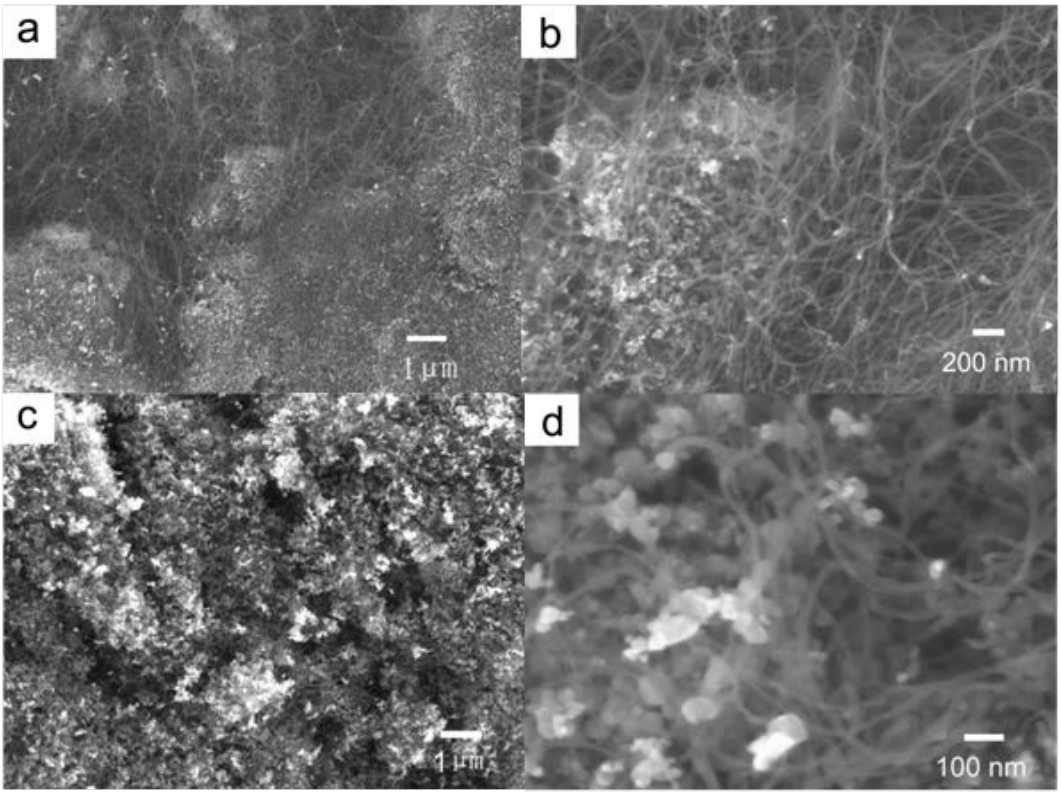

Figure 3. SEM images of carbon nanotubes prepared on (a, b) 5 wt% Cu and 5 wt% Mo and (c,d) 10 wt%Cu and 5 wt% Mo at 850 ºC for 1 h.

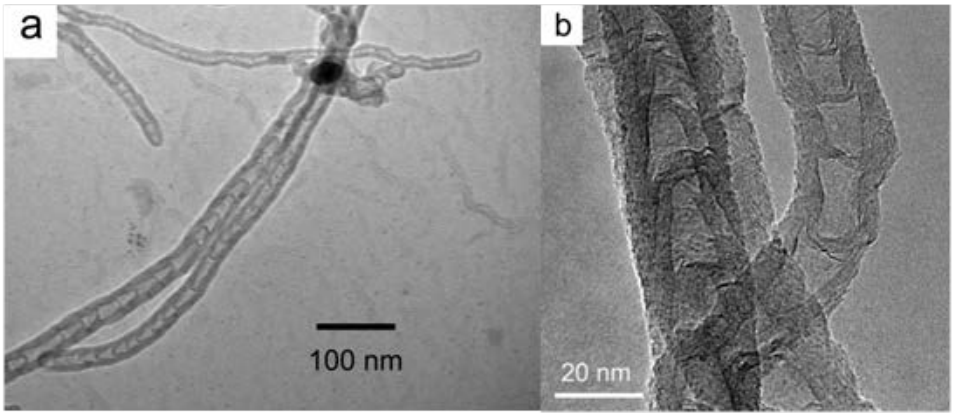

Figure 4. TEM images of bamboo-structured carbon nanotubes prepared by methane deposition over 10 wt% Cu and 5 wt% Mo at 850 ^{o}C for 1h.

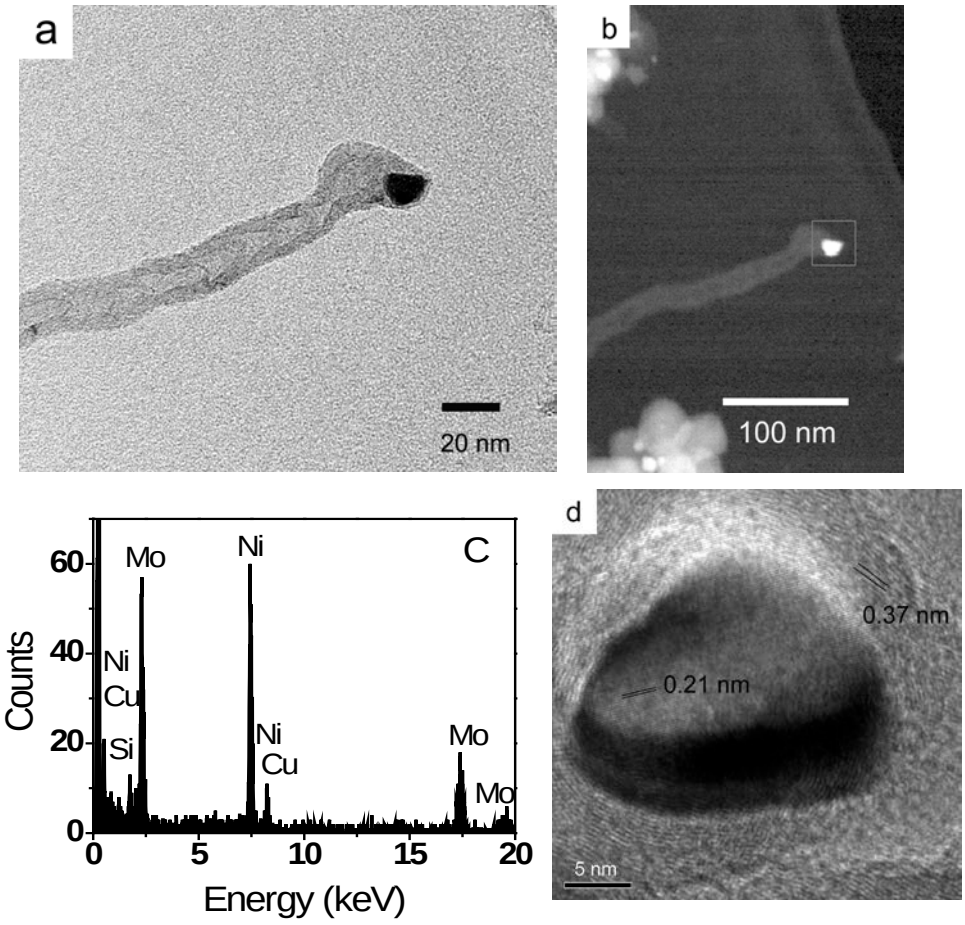

Figure 5. (a) Bright field and (b) dark field TEM images of a catalyst nanoparticle at the tip of a BCNT, (c) EDAX analysis of the catalyst nanoparticle and (d) HRTEM image of a catalyst nanoparticle (scale bar: 5 nm).

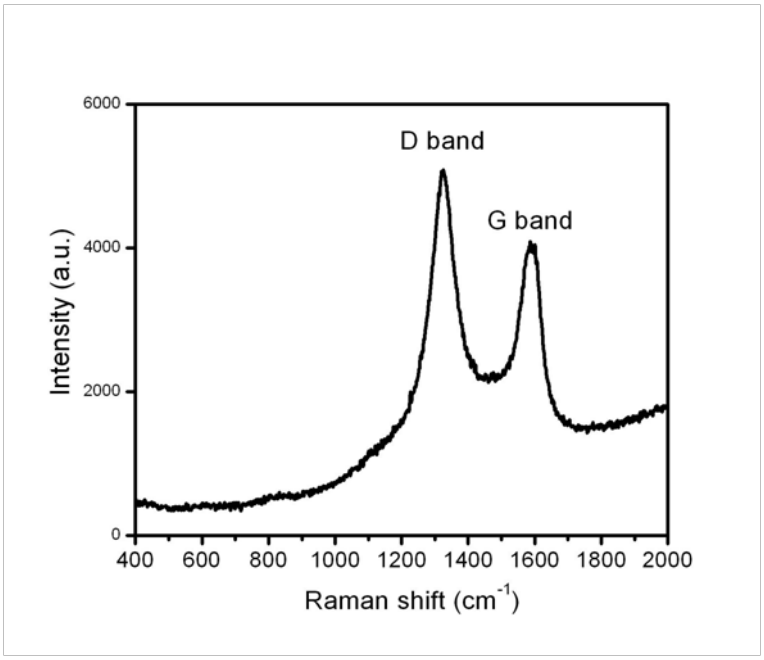

Figure 6. Raman spectrum of BCNTs after purification using 3 M HNO_3.

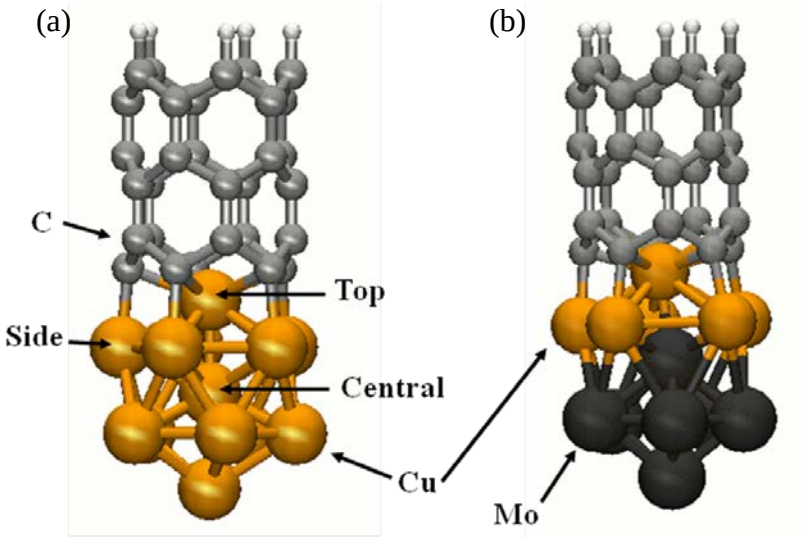

Figure 7 (a) Optimized structures of the M_{13} cluster – (5,0) SWNT complexes **I** (Cu_{13}) and (b) **III** (Mo_7Cu_6). Central, Side and Top marks the atoms replaced to construct the other composite Cu/Mo particles. Complex **II** contains only Mo (Mo_{13}). Replacing the central Cu atom of complex **I** by Mo gives complex **IV** ($MoCu_{12}$), while replacing the *side* or *top* Cu with Mo gives complexes **V** and **VI** ($MoCu_{12}$), respectively. For complex **VII** (Mo_8Cu_5) the corresponding *top* Cu of complex **III** has been replaced with Mo.